

Parent Porphyrin (Porphine) and its Complexes with 3d Metals

Jan Plutnar,^a Lucie Bednářová,^a Ivana Císařová,^b Martin Dračínský,^a Lenka Krepsová,^a Ján Tarábek,^a and Josef Michl^{a,c*}

^a *Institute of Organic Chemistry and Biochemistry of the Czech Academy of Sciences, Flemingovo nám. 2, 160 00, Prague*

^b *Charles University, Faculty of Science, Department of Inorganic Chemistry, Hlavova 8, 128 40, Prague 2, Czech Republic*

^c *Department of Chemistry, University of Colorado, Boulder, CO 80309, U.S.A.*

Abstract

We report an improved synthesis of porphine from *d*-tartaric acid, its conversion to complexes with Mg(II), V(IV), Mn(III), Fe(III), Co(II), Ni(II), Cu(II) and Zn(II), their IR, UV-vis, NMR, XPS, and mass spectra, and single crystal X-ray diffraction structures of *meso*-tetrakis(*n*-hexyloxycarbonyl)porphyrin and (porphyrinato)manganese(III) bromide.

Introduction

Recently, the two-dimensional fully conjugated polymer porphene (**1**), analogous to graphene but composed of fused porphyrin instead of fused benzene rings, was synthesized by a single-step oxidative polymerization of the Zn salt of parent porphyrin **2** (also known as porphine) on the surface of water, with K₂IrCl₆ as the oxidant.¹ The initially formed free-base **1** strongly doped with electron holes was reduced with NaI and subsequently converted to its zinc salt Zn-**1** and other metal salts of **1** by reaction with solutions of metal chlorides. The potentially very large family of metalloporphenes M-**1**, possibly carrying a variety of axial substituents, remains to be explored. Density functional calculations suggest very interesting properties for these polymers, including metallic conductivity in certain metal complexes and semiconductivity in others.²

Some of the natural next questions are to inquire (i) whether other metalloporphyrins M-**2** and other oxidizing agents could be used instead of Zn-**2** and K₂IrCl₆, possibly offering some advantages, and (ii) how the structural and spectroscopic properties of metalloporphenes M-**1** compare with those of monomeric metalloporphenes M-**2**. Such a study is hindered both by the quite high cost of commercial **2** and poor yields of its published syntheses, and by the rather incomplete and scattered literature information on the properties of parent M-**2**, many of which are unknown.

Presently, we report an improved synthesis of the starting material **2** and IR, UV-vis, NMR, XPS, and MS data for M-**2**, where the metal M is Mg(II), V(IV), Mn(III), Fe(III), Co(II), Ni(II), Cu(II) and Zn(II). We also report single crystal X-ray diffraction structures of *meso*-tetrakis(*n*-hexyloxycarbonyl)porphyrin (**3**) and (porphyrinato)manganese(III) bromide.

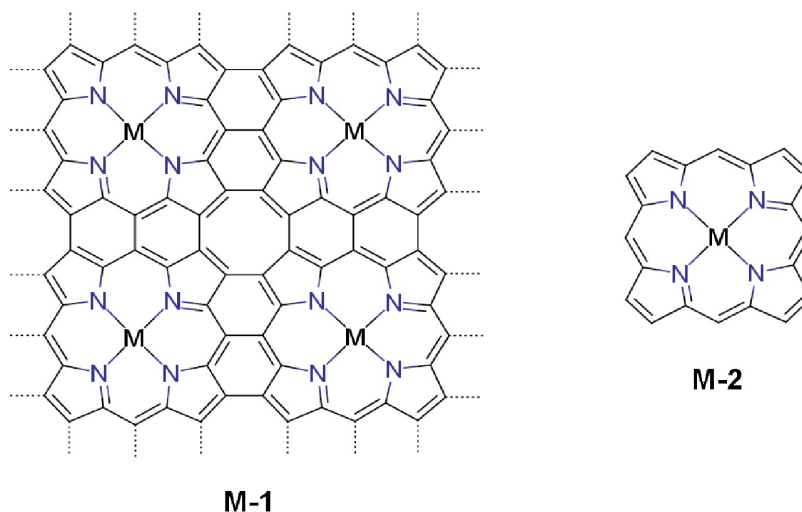
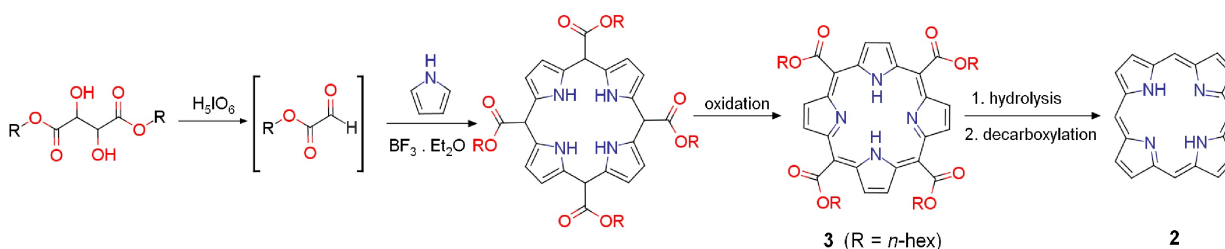


Chart 1. Structure of metalloporphene (M-1) and metalloporphine (M-2).

Results

Synthesis of Porphine (2). We followed the approach of Neya and Funasaki (Scheme 1)³ but introduced some modifications that improved the yield and made the reactions easier to perform.



Scheme 1. Preparation of porphine (**2**) via *meso*-tetrakis(alkyloxycarbonyl)porphyrins.

The initial step is oxidation of an alkyl tartrate with periodic acid to form a glyoxylate ester.⁴ The reaction mixture contains some water as a byproduct (also, the periodic acid is added as a dihydrate) and a significant amount of periodic and iodic acid, causing the formation of geminal diols and hemiacetal esters. According to ¹H NMR, the mixture contains only ~2 % of the desired aldehyde, in a monomeric or trimeric form. This is increased to ~30 % by addition of P₂O₅ and a 1 h heating to 50 °C (¹H NMR signal at ~9.4 ppm),⁵ but not further even upon extended heating or use of a higher temperature. We have used this mixture in subsequent reaction steps.

The final step of the porphyrin-forming process is dehydrogenation of the intermediate. Various oxidizing agents are commonly used, from atmospheric oxygen in Adler's reaction in

refluxing propionic acid¹¹ to *p*-chloranil or 2,3-dichloro-5,6-dicyanobenzoquinone (DDQ) under milder conditions.⁶ Polypyromethenes, the major side products, are usually easily separated, but the removal of the reduction products of the organic oxidizing agents requires tedious chromatography. We have replaced the organic oxidants with pyridinium chlorochromate, easily prepared from CrO₃, hydrochloric acid and pyridine. The products of its reduction are easily separated by adsorption on silica and the desired porphyrin is extracted with dichloromethane.

The pure product tends to crystallize in perfect large purple crystals. Single-crystal X-ray diffraction revealed a triclinic P-1 space group (Table 1). Two opposed hexyloxycarbonyl groups on each ring are oriented parallel to the plane of the nitrogen atoms and the other two are rotated by ~70° out of this plane (Figure 1).

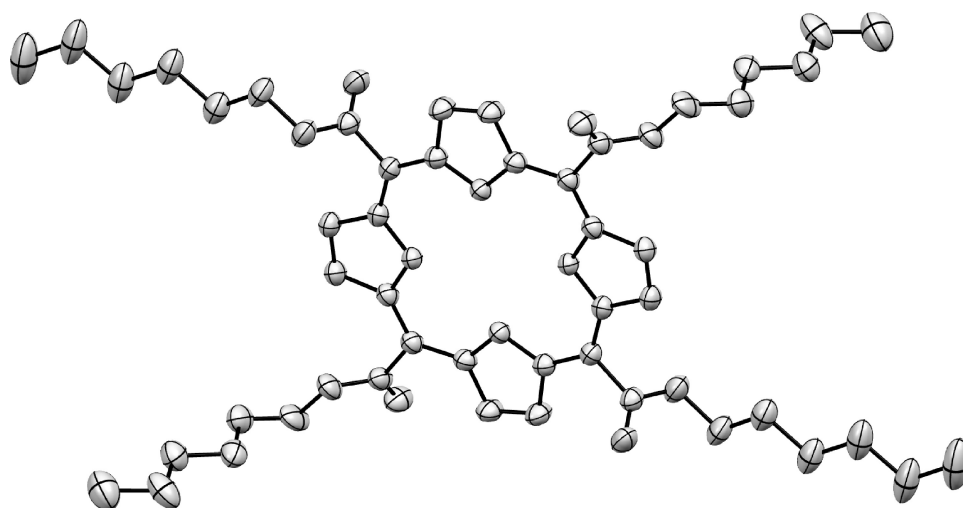


Figure 1. ORTEP image of **3** with 50% probability ellipsoids (hydrogen atoms were omitted for clarity).

Conversion of **3** into **2** requires hydrolysis followed by decarboxylation of the intermediate tetracarboxylic acid, and can be accomplished by heating in a concentrated sulfuric acid solution.³ However, even in the absence of oxygen, much of the porphyrin turns into a black tar and the yield rarely exceeded 60%. As an alternative, concentrated orthophosphoric acid effects the decarboxylation well, but it cannot be used to hydrolyze the ester. The original one-pot synthesis was therefore divided into two separate reaction steps. The first is an alkaline ester hydrolysis and the second is acidic decarboxylation. Both steps are almost quantitative and they can be carried out in the same flask.

With these modifications, the overall yield of **2** based on di-*n*-hexyl tartrate is 10 - 15%.

Table 1. - Crystallographic parameters of **3** and MnBr-**2**.

	3	MnBr- 2
Formula	C ₄₈ H ₆₂ N ₄ O ₈	C ₂₀ H ₁₂ BrMnN ₄
M.w.	823.01	443.19
Crystal system	triclinic	monoclinic
Space group	$P\bar{1}$	P2 ₁ /n
<i>a</i> [Å]	8.1289(6)	11.0421(3)
<i>b</i> [Å]	10.0463(7)	9.2418(3)
<i>c</i> [Å]	14.4948(10)	17.1840(4)
α [deg]	72.502(3)	90
β [deg]	89.279(4)	101.4690(10)
γ [deg]	80.146(3)	90
<i>Z</i>	1	4
<i>V</i> [Å ³]	1111.34(14)	1718.59(8)
Temperature [K]	150	120
Wavelength [Å]	1.54178	0.71073
ρ [g cm ⁻³]	1.230	1.713
Crystal size [mm]	0.19 × 0.11 × 0.09	0.26 × 0.20 × 0.20
Crystal color, shape	dark red-blue, prism	dark red, prism
μ [mm ⁻¹]	0.67	3.10
<i>T</i> _{min} , <i>T</i> _{max}	0.82, 0.94	0.49, 0.58
Measured reflections	18206	32591
Independent diffract. ions (<i>R</i> _{int})	4343 (0.061)	3929 (0.029)
Observed diffractions [<i>I</i> >2 σ (<i>I</i>)]	3712	3823
No. of parameters	313	235
<i>R</i>	0.069	0.030
<i>wR</i> (<i>F</i> ²) for all data	0.182	0.070
GOF	1.06	1.096
Residual electron density [e/Å ³]	0.59, -0.30	0.59, -1.36
goodness-of-fit	1.057	1.096

Synthesis of Metalloporphines (M-2). Standard procedures were used successfully. Treatment **2** with MgH_2 in boiling dry pyridine afforded a yield of 85% after chromatography. Against our expectations,⁷ the ^1H NMR spectrum revealed no Mg-coordinated pyridine. In contrast, an analogous reaction of **2** with Zn(II) acetate afforded zinc(II) porphyrin (Zn-**2**) as a 1:1 adduct with pyridine, whose *o*-, *m*- and *p*- protons were shifted upfield by 4.55, 1.67 and 1.31 ppm, respectively. Free square-planar Zn-**2** was prepared either by heating the pyridine adduct at 200 °C under reduced pressure overnight or by heating **2** with Zn(II) acetate in benzonitrile. Cu(II), Co(II), Ni(II) and VO(II) porphyrins were obtained in good yield by heating porphine with a metal(II) acetate or vanadyl(II) sulfate in benzonitrile close to the boiling point overnight. Pyridine and *N,N*-dimethylformamide can also be used, but the yields are usually lower.

The reaction with Co(II) was performed in the dark under exclusion of oxygen. So was the reaction of porphine with FeCl_2 , which produced a moderate yield of (porphyrinato)iron(III) chloride instead of Fe(II) porphine, as expected.⁸ (Porphyrinato)manganese(III) chloride and bromide were obtained by a room temperature reaction of porphine and the manganese(II) halide in benzonitrile in the presence of sodium acetate. The crystal structure of (porphyrinato)manganese(III) bromide is square pyramidal, with the manganese atom displaced 0.225 Å out of the plane of the nitrogen atoms. The beta carbons of the porphine ligand are displaced by ~0.1 Å in the opposite direction, giving the molecule the shape of an inverted umbrella (Figure 2).

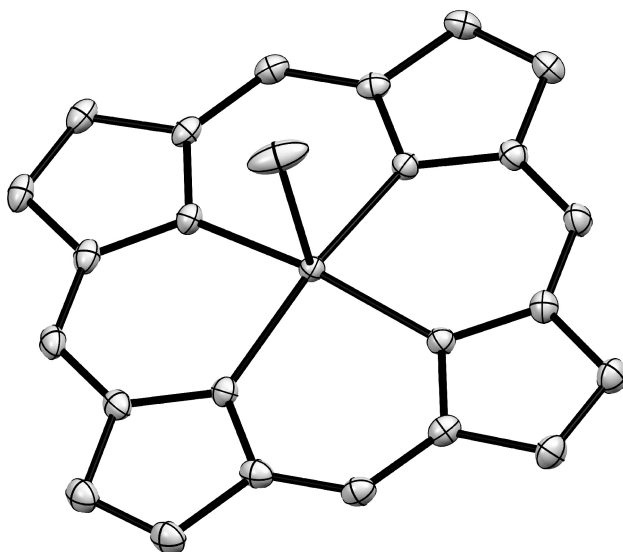


Figure 2. ORTEP image of MnBr-**2** with 50% probability ellipsoids (hydrogen atoms were omitted for clarity).

The metalloporphyrins were characterized by IR (Table S1 and Figures S... - S...), UV-vis (Table S3 and Figures 3 - 10), NMR (Table 2 and Figures S... - S.. Wi.) XPS (Table 3 and Figures S... - S...), and MS.

Discussion

Porphine (2) and Metalloporphine (M-2) Synthesis. Efforts to synthesize the porphyrin macrocycle were started by Hans Fischer over a century ago.⁹ Two decades later, Rothmund's cyclocondensation procedure¹⁰ represented an important advance, but the yields remained extremely low. Many others contributed, and particularly noteworthy are Adler and Longo's condensation of pyrrole with an aldehyde in refluxing propionic acid¹¹ and Lindsey's acid catalyzed cyclization.¹² Although fairly successful for substituted porphyrins, these procedures yield only minimal yields of parent **2**, on the order of 1 - 2%.¹³ Oxidation of 2-hydroxymethylpyrrole solutions with potassium persulfate affords a yield of ~5% but appears unsuitable for a preparation of larger amounts of **2**.¹⁴

We have adopted the more recently developed procedure of Neya and Funasaki, who prepared **2** by thermal removal of meso substituents from protonated *meso*-tetrakis(*t*-butyl)porphyrin¹⁵ and *meso*-tetrakis(*n*-hexyloxycarbonyl)porphyrin (**3**)³ in ~75% yield. These meso substituted porphyrins have been reported to form in yields of ~15% from readily available starting materials^{16,17} (Scheme 1). Unfortunately, in our hands the yields of **3** prepared according to the published procedure fluctuated considerably and never exceeded ~10% (based on di-*n*-hexyl tartrate). They were even lower when the alkyl R was *n*-butyl or *n*-octyl instead of *n*-hexyl. The modified procedure developed presently reliably converts di-*n*-hexyl tartrate into **2** in an overall yield of 10 - 15%.

The improved availability of **2** permitted us to prepare metalloporphines containing magnesium and all 3*d* metals except titanium in quantities adequate for a thorough spectroscopic characterization. Since we expect to use these compounds for oxidative polymerization on the surface of water, we have chosen higher oxidation states of the metal when there was a choice.

Magnesium(II) porphyrin (Mg-**2**) was prepared previously in nearly quantitative yield from **2** and MgBr₂·Et₂O in the presence of a base¹⁸ and in 40% yield by Mg-salt assisted self-condensation of 1-formyldipyromethane.¹⁹ Several methods of preparation of zinc(II) porphine (Zn-**2**) were reported, mostly consisting of a reaction between porphine and zinc(II) acetate in a suitable solvent^{13,20} (THF, CH₂Cl₂/MeOH). Copper(II) porphine (Cu-**2**) is one of the earliest examples of an artificial metalloporphyrin. It was prepared from copper(II) acetate and porphine in boiling acetic acid by Rothmund in 1936.¹⁰ It was also prepared by reaction of bis(acetylacetonato)copper(II) with porphine in refluxing chloroform.²¹ Nickel(II) porphyrin (Ni-**2**) was previously prepared in an unreported yield by refluxing nickel(II) acetate and porphyrin in chloroform.²² Cobalt(II) porphine (Co-**2**) was prepared in a moderate yield using a transmetallation reaction of magnesium(II) porphine and cobalt(II) acetate in hot benzonitrile.²³ A preparation of the (porphyrinato)iron(III) chloride complex with a relatively high yield (75 %) was reported, using a reaction between porphine and iron(II) chloride in refluxing *N,N*-dimethylformamide.⁸

Vibrational Spectra (Tables S1 and S2, Figures S... - S...). The IR spectra recorded for the Mg(II), Zn(II), Cu(II) and Ni(II)-porphyrins correspond to those already reported.^{24,25} The IR spectra of all M-**2** metalloporphines show a similar signal pattern with only minor differences in frequencies of some of the bands. When compared to the spectrum of **2** itself, the most notable differences are (i) the absence of signals that **2** has at 718, 728 and 970 cm⁻¹ spectrum, assigned to the in- and out-of-plane bending vibrations of the pyrrole rings^{24,26} and (ii) a significant change of the frequencies of the bands assigned to the in- and out-of-plane bending modes of the meso C-H bond,²⁴ which move from 950 and 1224 cm⁻¹ in **2** to 991-1003 and 1289-1318 cm⁻¹ in

M-2, respectively.

UV-vis Absorption Spectra (Table S3 and Figures 3 - 10). The electronic absorption spectra of **M-2** metalloporphyrins without an axial ligand (D_{4h} symmetry) are dominated by a weak Q band carrying fine structure and by a very strong Soret band. Those metalloporphyrins with an axial ligand (C_{4v} symmetry) are much more complex. This is attributable to an interaction of $3d$ orbitals of the metal dication with the π -electron system of the porphyrin dianion and the presence of ligand-to-metal charge transfer bands in the spectrum. For six of the metalloporphyrins, the situation has been analyzed in considerable detail elsewhere.²

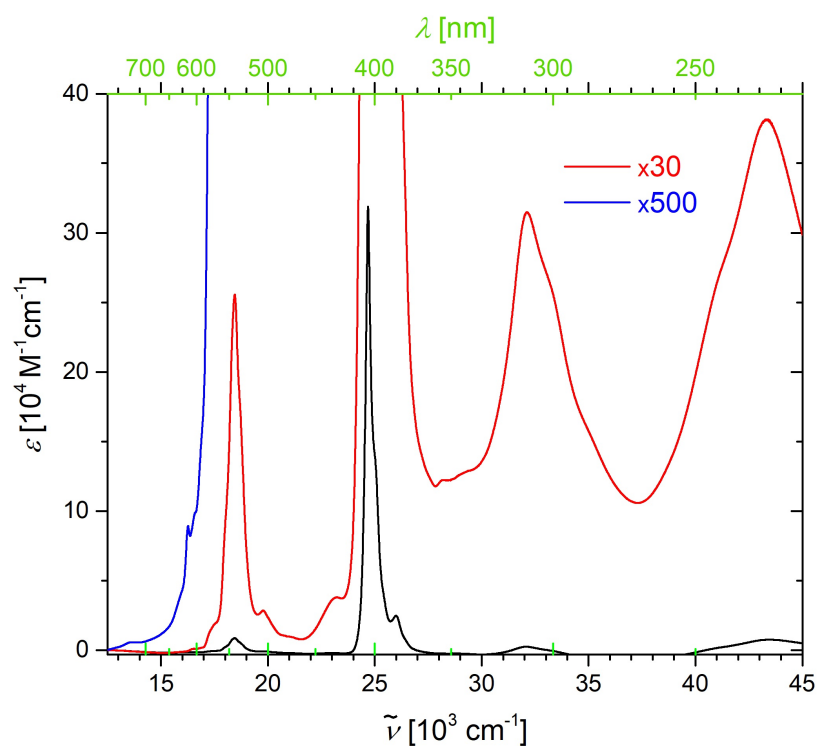


Figure 3 - UV-vis absorption spectrum of **Mg-2** in THF.

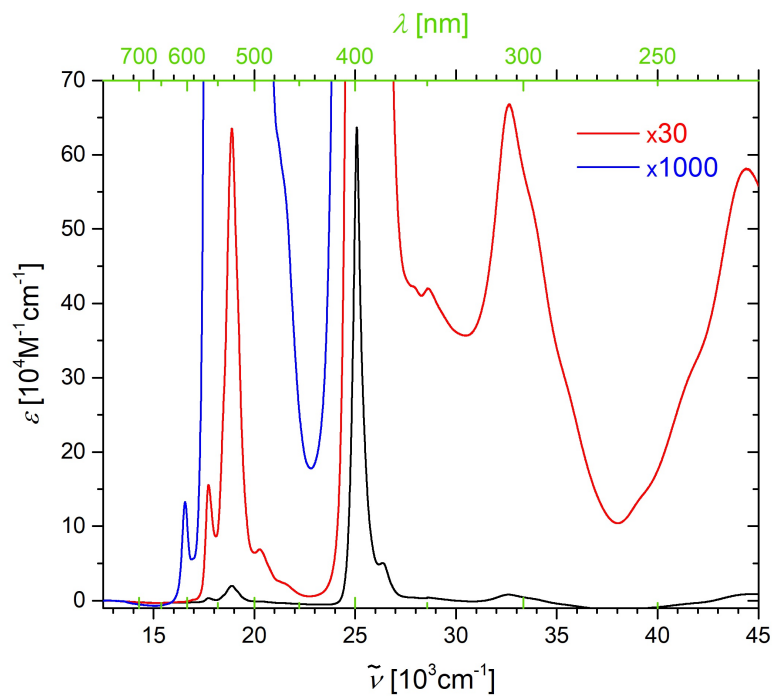


Figure 4 - UV-vis absorption spectrum of Zn-2 in THF.

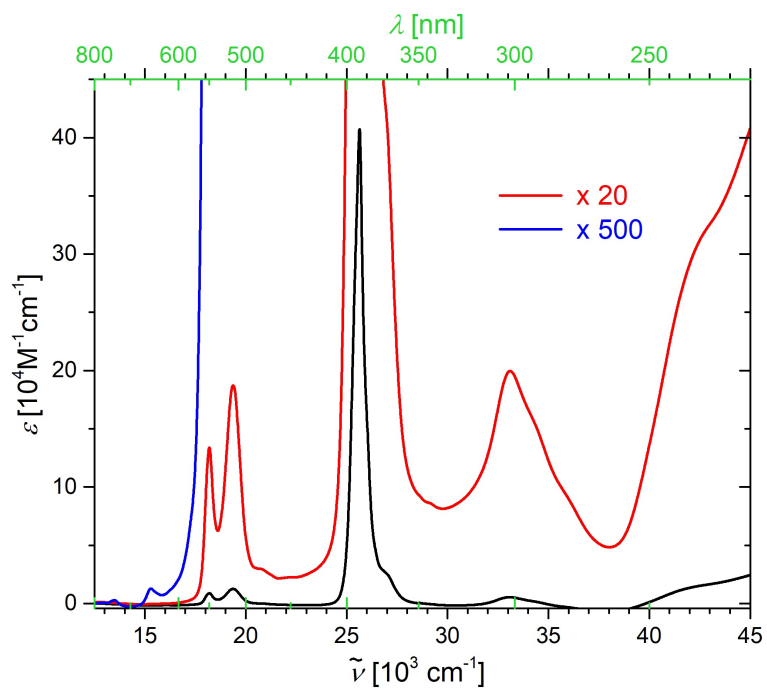


Figure 5 - UV-vis absorption spectrum of Cu-2 in THF.

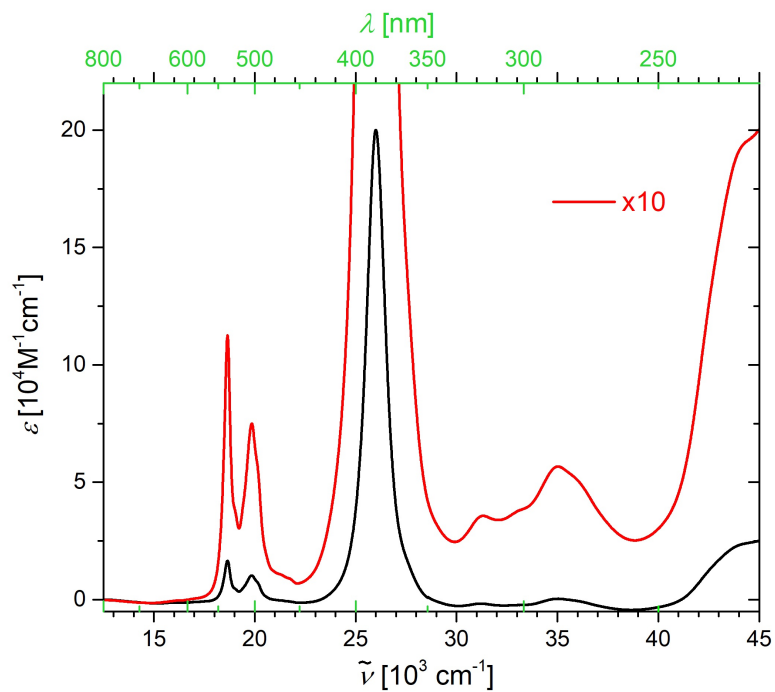


Figure 6 - UV-vis absorption spectrum of Ni-2 in THF.

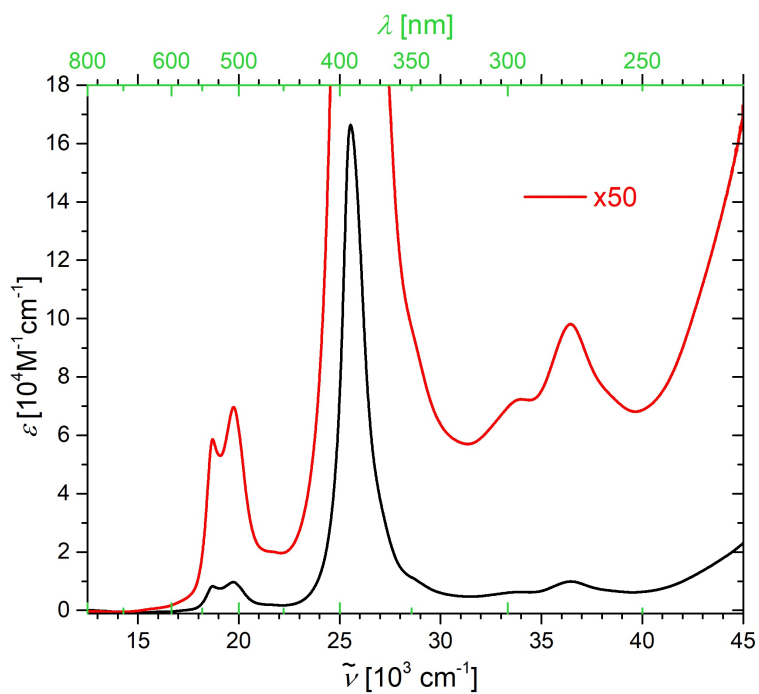


Figure 7 - UV-vis absorption spectrum of Co-2 in THF.

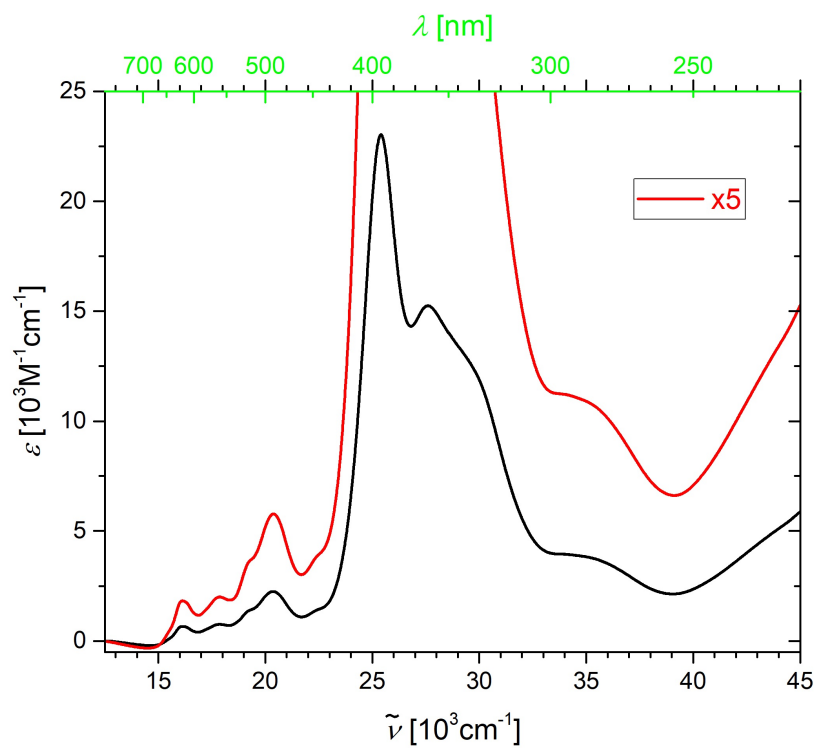


Figure 8 - UV-vis absorption spectrum of FeCl-2 in THF.

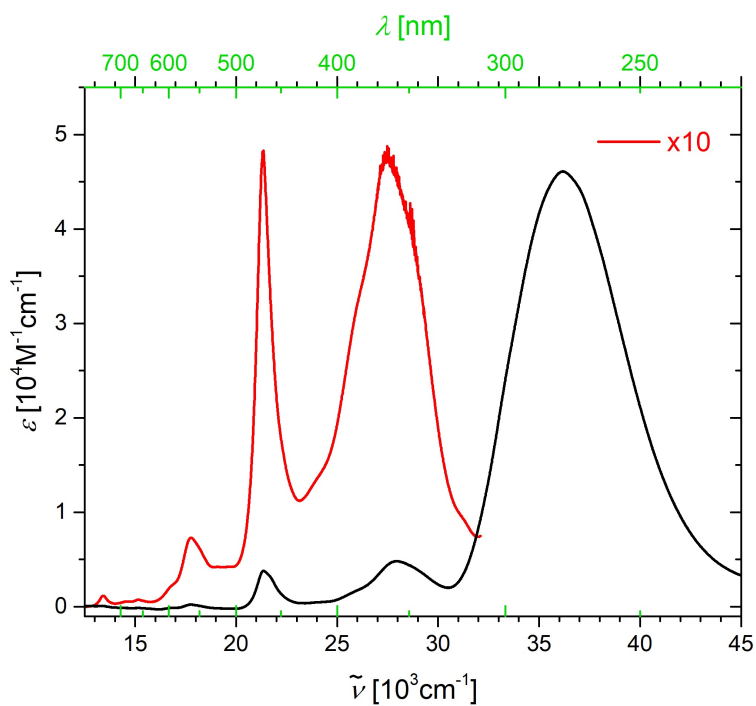


Figure 9 - UV-vis absorption spectrum of MnBr-2 in THF.

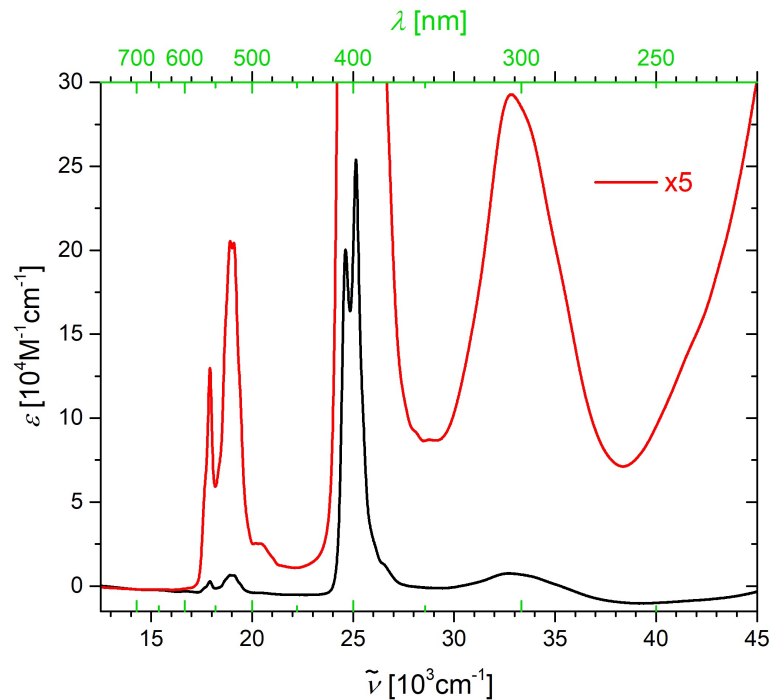


Figure 10 - UV-vis absorption spectrum of VO-2 in THF.

Nuclear Magnetic Resonance (NMR, Table 2 and Figures S... - S...). ^1H , ^{13}C and ^{15}N spectra were observed for all the M-2 metalloporphyrins, except the Cu(II), Co(II) and VO(II) salts. Only small variation was found in the chemical shifts of the meso and the β protons of the diamagnetic Mg(II), Zn(II) and Ni(II) salts. The ^1H NMR signals of the β protons of the Mn(III) and Fe(III) complexes exhibit significant paramagnetic shifts, and those of the Mn(III) salts also a substantial paramagnetic line broadening, when compared to the diamagnetic analogues (e.g., the

FWHM of the β protons is ~ 0.6 Hz in Zn-2 and 463 Hz in MnCl-2.

Direct acquisition of the ^{15}N NMR chemical shifts would require the preparation of isotopically labeled metalloporphyrins²⁷ and we determined them from (^1H , ^{15}N) HMBC correlation spectra. They are in the range 190-207 ppm in 2, Mg-2, and Zn-2, but the value for Ni-2 is 123.1 ppm, suggesting the presence of a rapid equilibrium in which a fraction of the molecules is in the triplet state.

Table 2 - The ^1H and ^{15}N NMR chemical shifts of the prepared compounds

signal [ppm]	3	2	Mg-2	Zn-2	Ni-2	MnBr-2	FeCl-2
<i>meso</i>	N/A	10.64	10.42	10.34	10.38	n.d.	50.9 [‡]
β	9.55	9.76	9.59	9.55	9.56	-30.9*	52.2 [‡]
N-H	-3.36	-4.16	N/A	N/A	N/A	N/A	N/A
^{15}N	n.d.	189.8	206.2	203.8	123.1	n.d.	n.d.

* the FWHM values of the signals are 463 and 437 Hz for the MnClP and MnBrP complexes, respectively; ‡ in CD_3OD at 5 °C, FWHM 193 and 165 Hz, respectively

X-Ray Photoelectron Spectra (XPS, Table 3 and Figures S... - S...). In order to be able to

Table 3 - Binding energies of the N 1s electrons in the prepared compounds.

Compound	E_b [eV]
3 ^a	397.9; 400.2
2 ^a	399.0
Mg-2	399.4
Zn-2	400.4
Cu-2	399.8
Ni-2	396.9
Co-2	397.4
FeCl-2	397.8
MnBr-2	398.5
VO-2	399.5

observe the changes in the electron distribution in porphene compared to the compounds it is prepared from in solid state, the high resolution spectra of the core N 1s region of the compounds were recorded.

Summary

(i) By modifying the reported synthetic procedures, the yield of 2 and the ease of performing the reactions have been improved. The improved synthesis starts with tartaric acid and 1-hexanol and involves five reaction steps. It requires no lengthy chromatography and the overall yield is 10-15% based on di-*n*-hexyl tartrate. Batches of ~ 1 g can be prepared without difficulties.

(ii) Metalloporphyrins containing Mg and most of the 3d metals have been prepared and their IR, UV-vis, NMR, XPS, and MS spectra have been measured.

(iii) Single-crystal X-ray diffraction structures

of *meso*-tetrakis(*n*-hexyloxycarbonyl)porphyrin (**3**) and (porphyrinato)manganese(III) bromide have been obtained.

Experimental Part

Di-*n*-hexyl *d*-Tartrate. *d*-Tartaric acid (20 g), *n*-hexanol (150 mL) and *p*-toluenesulfonic acid hydrate (2 g) were mixed in a round-bottomed flask (250 mL) equipped with a Dean-Stark apparatus capped with a CaCl₂-filled drying tube. The reaction mixture was heated to 200 °C and refluxed until all water produced during the reaction has been removed. After cooling to room temperature, the unreacted *n*-hexanol was removed by vacuum distillation. The cold yellowish distillation residue was poured into a saturated aqueous NaHCO₃ solution and extracted with dichloromethane. The collected organic phases were dried over Na₂SO₄ and the solvent removed under reduced pressure to yield the product as a yellowish oil (39.5 g, 93 %). ¹H NMR (CDCl₃) δ 0.88 (m, 6H), 1.26-1.39 (m, 12H), 1.64-1.71 (m, 4H), 3.21 (d, 7.7 Hz, 2H), 4.24 (m, 4H), 4.52 (d, 7.7 Hz, 2H); ¹³C NMR (CDCl₃) δ 171.6, 72.0, 66.5, 31.3, 28.4, 25.3, 22.4, 13.9.

5,10,15,20-Tetrakis(*n*-hexyloxycarbonyl)porphyrin (3**).** Di-*n*-hexyl tartrate (6 g) was dissolved in diethyl ether (200 mL), cooled with ice to 0 °C and periodic acid dihydrate (4.5 g) was added in small portions over 60 min. The resulting slurry was stirred in the melting ice-bath overnight. The ethereal solution was extracted with water (3 x 300 mL), dried over Na₂SO₄, and evaporated under reduced pressure. The oily residue was dissolved in dry hexane (100 mL) and phosphorus oxide (~ 6 g) was added in several portions with intense stirring. The mixture was heated to 50 °C and stirred under Ar atmosphere for 60 min. The solvent was cannulated into a pre-dried flask and evaporated under reduced pressure. The greenish-yellow oil was immediately used in the subsequent step.

A 6-L three-necked flask shielded from light was been loaded with freshly dried CH₂Cl₂ (4 L), freshly distilled pyrrole (2.7 mL), and the greenish oil from the previous step diluted with 100 mL of dry CH₂Cl₂. The flask was been flushed with argon and BF₃·Et₂O (0.8 mL) was added dropwise into the heavily stirred reaction mixture. The solution was stirred under inert atmosphere in the dark for 90 min. The Ar flow was stopped and pyridinium chlorochromate (9 g) was added at once. The resulting slurry was stirred in the dark overnight. The solvent was evaporated under reduced pressure in a 2 L flask. Silica (~ 400 mL) was added into the last evaporation batch and the mixture was evaporated to dryness.

Fresh silica was loaded onto a 21 cm wide Büchner funnel with a frit to form a layer approximately 6 cm thick. The silica containing the evaporated reaction mixture was loaded on top of this layer and washed with CH₂Cl₂ until colorless. The purple eluate was collected and concentrated under reduced pressure. Hexane (300 mL) was added to the concentrated solution (100 mL) of the product and left to crystallize overnight. The resulting deep purple crystals were collected by filtration, washed with hexanes, and dried under reduced pressure to yield between 0.8 and 1.2 g of product (10-15 % yield). Crystals suitable for single-crystal X-ray diffraction were isolated by slow diffusion of hexane vapors into a saturated solution of the compound in CH₂Cl₂. ¹H NMR (CD₂Cl₂) δ (ppm) -3.36 (s, 2H), 0.95 (t, 7.2 Hz, 12H), 1.38-1.54 (m, 16H), 1.66-1.74 (m, 8H), 2.16 (dq, 7.9, 6.8 Hz, 8H), 5.06 (t, 6.8 Hz, 8H), 9.55(s, 8H). ¹³C NMR (CDCl₃) δ (ppm) 170.8, 131.6, 112.4, 67.9, 31.7, 29.2, 26.1, 22.8, 14.21. UV-vis (DMSO) λ [nm] 408, 505, 539, 580, 635. IR (KBr) $\tilde{\nu}$ [cm⁻¹] 687, 729, 769, 783, 798, 811, 835, 882, 907, 983, 1036, 1063, 1124, 1155, 1174, 1202, 1225, 1254, 1266, 1279, 1301, 1313, 1348, 1374, 1390,

1402, 1432, 1443, 1453, 1466, 1522, 1545, 1566, 1717.

Porphine (2). The product of the previous step (**3**, 500 mg) was dissolved in a mixture of THF and methanol (130 + 110 mL). KOH (5 g) dissolved in distilled water (50 mL) was added to the solution and the mixture was refluxed overnight. The color of the reaction mixture changed from deep purple-brown to reddish-violet. The reaction mixture was cooled to room temperature and neutralized with 10% HCl (40 mL). The solution was decanted and evaporated to dryness. To the dried residue, H₃PO₄ (80 mL) followed by P₄O₁₀ (5 g) were added, the flask was flushed with argon and heated to 200 °C for 4 h. The originally deep green solution changed to intense purple color. After cooling to room temperature, the mixture was carefully poured to a solution of Na₂CO₃ (120 g) in water (500 mL) in a 2 L Erlenmeyer flask. The brownish slurry was subsequently extracted with CHCl₃ (1 L), the extract was dried with Na₂SO₄ and evaporated to dryness to yield copper-colored powder (180 mg, 95 % yield). ¹H NMR (DMSO-*d*₆) δ (ppm) -4.16 (s, 2H), 9.76 (s, 4H), 10.64 (s, 8H). ¹³C NMR (DMSO-*d*₆) δ (ppm) 131.98, 104.24 (the third expected signal was not observed). ¹⁵N NMR (DMSO-*d*₆, H,N-HMBC, 80 °C) δ (ppm) 189.8. UV-vis (DMSO) λ [nm] 394, 488, 519, 560, 613. IR (KBr) $\tilde{\nu}$ [cm⁻¹] 640, 691, 717, 726, 743, 771, 794, 839, 852, 898, 949, 969, 1046, 1059, 1066, 1136, 1184, 1224, 1251, 1282, 1351, 1408, 1536, 1589.

Magnesium(II) Porphyrin (Mg-2). Porphine (**2**, 105 mg) was suspended in dry pyridine (50 mL) and magnesium hydride (500 mg) was added. The reaction mixture was refluxed at 140 °C under inert atmosphere for three days. The liquids were evaporated in vacuum, the solid residue was purified by column chromatography using a short column (~ 5 cm) of neutral alumina, and the product was eluted with a tetrahydrofuran/hexane (1 : 2) mixture. The pink fractions were evaporated, the residual solid was suspended in pentane, filtered and air-dried to yield 141 mg of a purple powder (85 %). ¹H NMR (acetone-*d*₆) δ (ppm) 9.59 (s, 8 H), 10.42 (s, 4H). ¹³C NMR (acetone-*d*₆) δ (ppm) 150.4, 132.9, 106.2. ¹⁵N NMR (DMSO-*d*₆, H,N-HMBC) δ (ppm) 206.2. UV-vis (THF) λ [nm] 230, 311, 384, 405, 432, 505, 542. HR-MS (APCI+) *m/z* calcd for C₂₀H₁₂N₄Mg: 332.0912; found: 333.0986 [M+H]⁺. Elemental analysis: calcd for C₂₀H₁₂N₄Mg: C, 73.4; H, 4.5; N, 17.1%. Found: C, 72.72; H, 4.33; N, 16.13%. IR (KBr) $\tilde{\nu}$ [cm⁻¹] 628, 708, 740, 767, 795, 850, 900, 991, 1050, 1149, 1216, 1261, 1289, 1318, 1356, 1388, 1408, 1486, 1512, 1539.

Zinc(II) Porphyrin (Zn-2). Porphine (**2**, 115 mg) and zinc(II) acetate (200 mg) were dissolved in freshly distilled benzonitrile (20 mL) and heated under argon atmosphere at 190 °C for 1 h. After cooling to room temperature, the reaction mixture was poured onto a short neutral alumina column and washed with dichloromethane to remove benzonitrile. The product was eluted with tetrahydrofuran. Purple crystals of the product precipitated upon concentration of the tetrahydrofuran solution under reduced pressure. The crystals were filtered, washed with a small amount of pentane and dried to yield 138 mg of the product (quant.). ¹H NMR (tetrahydrofuran-*d*₈) δ (ppm) 9.55 (s, 8H), 10.34 (s, 4H). ¹³C NMR (tetrahydrofuran-*d*₈) δ (ppm) 150.6, 132.7, 105.3. ¹⁵N NMR (tetrahydrofuran-*d*₈, H,N-HMBC) δ (ppm) 203.8. UV-vis (THF) λ [nm] 225, 307, 378, 398, 493, 530, 564, 604. HR-MS (ESI+) *m/z* calcd. for C₂₀H₁₂N₄Zn: 372.0353; found: 372.0351 [M⁺]. Elemental analysis: calcd. for C₂₀H₁₂N₄Zn.C₄H₈O: C, 64.7; H, 4.5; N, 12.6; Zn, 14.7 %. Found: C, 64.4; H, 4.3; N, 12.5; Zn, 14.8 %. IR (KBr) $\tilde{\nu}$ [cm⁻¹] 696, 739, 762, 798, 844, 990, 1051, 1150, 1298, 1383, 1429, 1465, 1489, 1515, 1548.

Copper(II) Porphyrin (Cu-2). Porphine (**2**, 30 mg), copper(II) acetate (60 mg) and dry benzonitrile (20 mL) were heated under argon atmosphere with exclusion of light at 180 °C for

60 min. After cooling to room temperature, the reaction mixture was poured on the top of a short (~5 cm) neutral alumina column; benzonitrile was removed with dichloromethane, and the product was eluted with tetrahydrofuran. The collected solutions were evaporated under vacuum to yield 30 mg of copper-colored powder (83 % yield). UV-vis (THF) λ [nm] 302, 371, 390, 515, 550, 653. HR-MS (ESI+) m/z calcd. for $C_{20}H_{12}N_4Cu$: 371.0358; found 372.0426 $[M+H]^+$. IR (KBr) $\tilde{\nu}$ [cm^{-1}] 696, 700, 731, 743, 801, 846, 858, 901, 949, 969, 995, 1018, 1056, 1151, 1223, 1245, 1308, 1351, 1530. Elemental analysis: calcd. for $C_{20}H_{12}N_4Cu \cdot \frac{1}{3}H_2O$: C, 63.6; H, 3.4; N, 14.8; Cu, 16.8%. Found: C, 63.8; H, 3.2; N, 14.4; Cu, 16.8%.

Nickel(II) Porphyrin (Ni-2). Porphine (**2**, 20 mg), nickel(II) acetate tetrahydrate (100 mg), and dry benzonitrile (20 mL) were refluxed with exclusion of light under an argon atmosphere at 200 °C for 2 h. After cooling to room temperature, the reaction mixture was poured on the top of a short (~5 cm) neutral alumina column. Benzonitrile was removed with dichloromethane and the product was eluted with tetrahydrofuran. The collected THF fractions were concentrated under reduced pressure and the product was precipitated with small amount of pentane. The resulting precipitate was filtered, washed in pentane, and dried under reduced pressure to yield 21 mg of a red powder (yield 89 %). 1H NMR (DMSO- d_6) δ (ppm) 9.56 (s, 8H), 10.38 (s, 4H). ^{13}C NMR (DMSO- d_6) δ (ppm) 142.7, 132.5, 104.4. ^{15}N NMR (DMSO- d_6 , H,N-HMBC) δ (ppm) 123.1. UV-vis (THF) λ [nm] 284, 302, 320, 384, 504, 536. HR-MS (ESI+) m/z calcd. for $C_{20}H_{12}N_4Ni$: 366.0415; found 367.0485 $[M+H]^+$. IR (KBr) $\tilde{\nu}$ [cm^{-1}] 699, 744, 769, 805, 854, 896, 995, 1036, 1060, 1066, 1151, 1251, 1318, 1386, 1462, 1546. Elemental analysis: calcd. for $C_{20}H_{12}N_4Ni \cdot \frac{1}{3}C_4H_8O$: C, 65.5; H, 3.8; N, 14.3; Ni, 15.0%. Found: C, 65.3; H, 3.3; N, 14.4; Ni, 14.6%.

Cobalt(II) Porphyrin (Co-2). Porphine (**2**, 30 mg), cobalt(II) acetate tetrahydrate (50 mg) and dry benzonitrile (20 mL) were heated with exclusion of light under an argon atmosphere at 140 °C overnight. After cooling to room temperature, the reaction mixture was purified on a short (~5 cm) neutral alumina column. Benzonitrile was removed with dichloromethane and the product was eluted with tetrahydrofuran. The collected fractions were concentrated under reduced pressure and the product was precipitated with a small amount of pentane. The solids were filtered, washed with pentane, and dried under reduced pressure to yield black crystalline powder (29 mg, 82 % yield). UV-vis (THF) λ [nm] 274, 295, 391, 507, 535, 604. HR-MS (ESI+) m/z calcd. for $C_{20}H_{12}N_4Co$: 367.0394; found 367.0386 $[M^+]$. IR (KBr) $\tilde{\nu}$ [cm^{-1}] 696, 702, 743, 770, 844, 858, 891, 995, 1059, 1149, 1250, 1315, 1381, 1457, 1540. Elemental analysis: calcd. for $C_{20}H_{12}N_4Co \cdot \frac{1}{3}C_4H_8O$: C, 65.5; H, 3.8; N, 14.3; Co, 15.1%. Found: C, 65.2; H, 3.4; N, 14.5; Co, 15.2%.

(Porphyrinato)iron(III) Chloride (FeCl-2). Porphine (48 mg), iron(II) chloride tetrahydrate (200 mg), sodium acetate (130 mg), and benzonitrile were heated at 170 °C under an argon atmosphere in the dark overnight. After cooling to room temperature, the reaction mixture was purified by chromatography on a neutral alumina column. Benzonitrile was removed with dichloromethane and the product was eluted with tetrahydrofuran, followed by a tetrahydrofuran/methanol (3:1) mixture, as a greenish-red solution. The collected fractions were evaporated under reduced pressure. The resulting black crystals were suspended in pentane, filtered and dried under reduced pressure to yield 34 mg of the product (55 %). UV-vis (THF) λ [nm] 287, 339, 362, 393, 445, 491, 517, 563, 621. MS (ESI+) m/z calcd. for $C_{20}H_{12}N_4Fe$: 364.04; found 364.0 $[M^+]$. IR (KBr) $\tilde{\nu}$ [cm^{-1}] 696, 706, 739, 775, 789, 797, 849, 860, 868, 912, 994,

1056, 1063, 1149, 1241, 1302, 1369, 1434, 1516. Elemental analysis: calcd. for $C_{20}H_{12}N_4Fe \cdot CH_3OH$: C, 58.4; H, 3.7; N, 13.0; Fe, 13.0%. Found: C, 58.2; H, 3.1; N, 12.8; Fe, 13.0%.

(Porphyrinato)manganese(III) Bromide (MnBr-2). Porphine (**2**, 30 mg), anhydrous manganese(II) bromide (70 mg), sodium acetate (100 mg), and benzonitrile (10 mL) were stirred in the dark under an argon atmosphere at 100 °C for 4 h. After cooling to room temperature, the reaction mixture was purified by chromatography on silica. Subsequent elution with dichloromethane and a mixture of dichloromethane with acetonitrile (3:1 - 1:1) resulted in separation of the product from benzonitrile and the other reaction products and impurities. The product crystallizes upon concentration of the deep-red solutions under reduced pressure as black shiny crystals which are collected by filtration, washed with diethyl ether and dried under reduced pressure (33 mg, 77 % yield). 1H NMR (MeOD) δ (ppm) -30.9 (s, β -H). The signal of the meso proton has not been observed. UV-vis (THF) λ [nm] 275, 363, 469, 562, 595, 659, 745. HR-MS (ESI+) m/z calcd. for $C_{20}H_{12}N_4Mn$: 363.0442; found 363.0428 [M^+]. IR (KBr) $\tilde{\nu}$ [cm^{-1}] 592, 619, 683, 701, 743, 776, 793, 801, 857, 873, 908, 1003, 1022, 1037, 1059, 1114, 1150, 1170, 1310, 1370, 1398, 1434, 1476, 1524, 1566. Elemental analysis: calcd. for $C_{20}H_{12}N_4MnBr$: C, 54.2; H, 2.7; N, 12.6; Mn, 12.4; Br, 18.0%. Found: C, 54.1; H, 2.8; N, 12.7; Mn, 11.5; Br, 16.8%.

Oxo(porphyrinato)vanadium(IV) (VO-2). Porphine (**2**, 30 mg), vanadyl sulphate pentahydrate (100 mg) and benzonitrile (10 mL) were refluxed in the dark under an argon atmosphere for 48 h. After cooling to room temperature, the reaction mixture was purified by chromatography on alumina using dichloromethane to remove benzonitrile, and tetrahydrofuran to elute the product. Violet needles of the product crystallized upon concentration of the collected THF fractions under reduced pressure. The crystals were collected by filtration, washed with diethyl ether, and dried under reduced pressure (34 mg, 94 % yield). UV-vis (THF) λ [nm] 303, 398, 406, 489, 523, 529, 558. HR-MS (ESI+) m/z calcd. for $C_{20}H_{12}N_4VO$: 375.0451; found 376.0526 [$M+H$] $^+$. IR (KBr) $\tilde{\nu}$ [cm^{-1}] 422, 664, 708, 734, 743, 767, 782, 802, 848, 868, 994, 1020, 1051, 1149, 1241, 1301, 1377, 1436, 1520, 1569. Elemental analysis: calcd. for $C_{20}H_{12}N_4VO$: C, 64.0; H, 3.2; N, 14.9; V, 13.6%. Found: C, 64.1; H, 3.2; N, 14.3; V, 12.8%.

Acknowledgement. This work was supported by Czech Science Foundation grant 20-03691X and Institute of Organic Chemistry and Biochemistry, RVO: 61388963.

References

1. Magnera, T. F.; Dron, P. I.; Bozzone, J. P.; Jovanovic, M.; Rončević, I.; Tortorici, E.; Bu, W.; Miller, E. M.; Rogers, C.; Michl, J. Porphene and Porphite as Porphyrin Analogs of Graphene and Graphite. *Nat. Commun.* **2023**, *14*, 6308.
2. Pavlak, I.; Matasovic, L.; Buchanan, E.; Michl, J.; Roncevic, I. Electronic Structure of Metalloporphenes, Antiaromatic Analogs of Graphene. ChemRxiv 2023, DOI: 10.26434/chemrxiv-2023-j0bv8-v2.
3. Neya, S.; Quan, J.; Hata, M.; Hoshino, T.; Funasaki, N. A Novel and Efficient Synthesis of Porphine. *Tetrahedron Letters*, **2006**, *47* (49), 8731–8732.

4. Kelly, T. R.; Schmidt, T. E.; Haggerty, J. G. A Convenient Preparation of Methyl and Ethyl Glyoxylate. *Synthesis*, **1972** (10), 544–545.
5. Christidis, Y. Verfahren zur Herstellung und Rueckgewinnung von Glyoxylsaeurehemiacetalestern in Verbesserten Ausbeuten. DE2811480 (A1), September 21, 1978.
6. Lindsey, J. S. The Synthesis of Meso-Substituted Porphyrins. In *Metalloporphyrins Catalyzed Oxidations*; Montanari, F., Casella, L., Eds.; Catalysis by Metal Complexes; Springer Netherlands: Dordrecht, **1994**; pp 49–86.
7. Devillers, C. H.; Dimé, A. K. D.; Cattey, H.; Lucas, D. *Crystallographic, Spectroscopic and Electrochemical Characterization of Pyridine Adducts of Magnesium(II) and Zinc(II) Porphine Complexes*. *Comptes Rendus Chimie* **2013**, *16* (6), 540–549.
8. Li, M.; Oliver, A. G.; Scheidt, W. R. *Characterization of Metalloporphines: Iron(II) Carbonyls and Environmental Effects on vCO*. *Inorg. Chem.* **2018**, *57* (9), 5648–5656.
9. Fischer, H.; Meyer, F.; *Zur Kenntnis der Porphyrinbildung, Hoppe-Seyler's Z. Physiol. Chem.*, **1912**, *82*, 97-108.
10. Rothmund, P. *A New Porphyrin Synthesis. The Synthesis of Porphin 1*. *J. Am. Chem. Soc.*, **1936**, *58* (4), 625–627.
11. Adler, A. D.; Longo, F. R.; Shergalis, W. Mechanistic Investigations of Porphyrin Syntheses. I. Preliminary Studies on Ms-Tetraphenylporphin. *J. Am. Chem. Soc.*, **1964**, *86* (15), 3145–3149.
12. Lindsey, J. S.; Hsu, H. C.; Schreiman, I. C. Synthesis of Tetraphenylporphyrins under Very Mild Conditions. *Tetrahedron Letters*, **1986**, *27* (41), 4969–4970.
13. Sun, Q.; Mateo, L. M.; Robles, R.; Ruffieux, P.; Lorente, N.; Bottari, G.; Torres, T.; Fasel, R. Inducing Open-Shell Character in Porphyrins through Surface-Assisted Phenalenyl π -Extension. *J. Am. Chem. Soc.*, **2020**, *142* (42), 18109–18117.
14. Krol, S. Notes- A New Synthesis of Porphin. *J. Org. Chem.*, **1959**, *24* (12), 2065–2067.
15. Neya, S.; Funasaki, N. Meso-Tetra(Tert-Butyl)Porphyrin as a Precursor of Porphine. *Tetrahedron Letters*, **2002**, *43* (6), 1057–1058.
16. Senge, M. O.; Bischoff, I.; Nelson, N. Y.; Smith, K. M. Synthesis, Reactivity and Structural Chemistry of 5,10,15,20-Tetraalkylporphyrins. *J. Porphyrins Phthalocyanines*, **1999**, *03* (02), 99–116.
17. Trova, M. P.; Gauuan, P. J. F.; Pechulis, A. D.; Bubb, S. M.; Bocckino, S. B.; Crapo, J. D.; Day, B. J. Superoxide Dismutase Mimetics. Part 2: Synthesis and Structure–Activity Relationship of Glyoxylate- and Glyoxamide-Derived Metalloporphyrins. *Bioorganic &*

Medicinal Chemistry, **2003**, *11* (13), 2695–2707.

18. Shi, D.-F.; Wheelhouse, R. T. *A Novel, High-Yielding Synthesis of Meso-Substituted Porphyrins via the Direct Arylation of Porphine*. *Tetrahedron Letters* **2002**, *43* (51), 9341–9342.
19. Dogutan, D. K.; Ptaszek, M.; Lindsey, J. S. *Direct Synthesis of Magnesium Porphine via 1-Formyldipyrromethane*. *J. Org. Chem.* **2007**, *72* (13), 5008–5011.
20. Zhang, Y.-H.; Zhao, W.; Jiang, P.; Zhang, L.-J.; Zhang, T.; Wang, J. *Structural Parameters and Vibrational Spectra of a Series of Zinc Meso-Phenylporphyrins: A DFT and Experimental Study*. *Spectrochimica Acta Part A: Molecular and Biomolecular Spectroscopy* **2010**, *75* (2), 880–890.
21. Wakui, Y.; Imura, H.; Suzuki, N. *Partition Coefficient of 21H,23H-Porphine and Its Metal(II) Complexes between Heptane and Nonaqueous Polar Solvents*. *BCSJ* **1991**, *64* (6), 2024–2026.
22. Unger, E.; Bobinger, U.; Dreybrodt, W.; Schweitzer-Stenner, R. *Vibronic Coupling in Nickel(II) Porphine Derived from Resonant Raman Excitation Profiles*. *J. Phys. Chem.* **1993**, *97* (39), 9956–9968.
23. Hatay, I.; Su, B.; Li, F.; Méndez, M. A.; Khoury, T.; Gros, C. P.; Barbe, J.-M.; Ersoz, M.; Samec, Z.; Girault, H. H. *Proton-Coupled Oxygen Reduction at Liquid–Liquid Interfaces Catalyzed by Cobalt Porphine*. *J. Am. Chem. Soc.* **2009**, *131* (37), 13453–13459.
24. Ogoshi, H.; Saito, Y.; Nakamoto, K. *Infrared Spectra and Normal Coordinate Analysis of Metalloporphins*. *J. Chem. Phys.* **1972**, *57* (10), 4194–4202.
25. Jarzecky, A. A.; Kozlowski, P. M.; Pulay, P.; Ye, B.-H.; Li, X.-Y. *Scaled Quantum Mechanical and Experimental Vibrational Spectra of Magnesium and Zinc Porphyrins*. *Spectrochim. Acta Part A: Molecular and Biomolecular Spectroscopy* **1997**, *53* (8), 1195–1209.
26. Mason, S. F. 196. *The Infrared Spectra of N-Heteroaromatic Systems. Part I. The Porphins*. *J. Chem. Soc.* **1958**, No. 0, 976–982.
27. Gust, D.; Roberts, J. D.; *Nitrogen-15 Nuclear Magnetic Resonance Studies of Porphyrins*. *J. Am. Chem. Soc.* **1977**, *99* (11), 3637–3640.